Available online at www.sciencedirect.com
ScienceDirect
Acta Biomaterialia 5 (2009) 1319–1327
Acta BIOMATERIALIA
www.elsevier.com/locate/actabiomat

Fabrication of HA/TCP scaffolds with a graded and porous structure using a camphene-based freeze-casting method

A. Macchetta, I.G. Turner *, C.R. Bowen

Department of Mechanical Engineering, University of Bath, Bath BA2 7AY, UK

Received 15 September 2008; received in revised form 14 November 2008; accepted 19 November 2008
Available online 6 December 2008

Abstract

A room temperature camphene-based freeze-casting method was used to fabricate hydroxyapatite/tricalcium phosphate (HA/TCP) ceramic scaffolds. By varying the solid loading of the mixture and the freezing temperature, a range of structures with different pore sizes and strength characteristics were achieved. The macropore size of the HA/TCP bioceramics was in the range of 100–200 μm, 40–80 μm and less than 40 μm at solid loadings of 10, 20 and 30 vol.%, respectively. The initial level of solid loading played a primary role in the resulting porosity of the scaffolds. The porosity decreased from 72.5 to 31.4 vol.% when the solid loading was increased from 10 to 30 vol.%. This resulted in an increase in the compressive strength from 2.3 to 36.4 MPa. The temperature gradient, rather than the percentage porosity, influenced the pore size distribution. The compressive strength increased from 1.95 to 2.98 MPa when samples were prepared at 4 °C as opposed to 30 °C. The results indicated that it was possible to manufacture porous HA/TCP bioceramics, with compressive strengths comparable to cancellous bone, using the freeze-casting manufacturing technique, which could be of significant clinical interest.

Keywords: Freeze-casting; Porous; Hydroxyapatite; Bioceramics

1. Introduction

Calcium phosphate-based bioceramics have received considerable attention as bone graft substitutes because of their excellent biocompatibility, bioactivity and osteoconductive characteristics compared to other materials. One of these bioceramics is hydroxyapatite (HA), which has a similar chemical composition to the major inorganic component of the skeletal tissue of vertebrates. It has been shown that synthetic HA is totally biocompatible, nontoxic and osteoconductive [1–3]. However, although HA is bioactive, it exhibits slow osteoconduction in vivo [1]. In the last decade, attention has focused on producing highly porous HA/TCP in either block or granular form in order to promote tissue ingrowth, thus enhancing the implant-tissue attachment and improving osteoinduction [4].

It has been reported that an optimal pore size exists for successful cell infiltration and host tissue ingrowth: 5–15 μm for fibroblasts, 20–125 μm for adult mammalian skin tissues and 100–350 μm for bone tissues [5]. There is also some evidence that pore interconnectivity is as important as porosity for bone ingrowth, particularly in the early stages of bone regeneration and penetration in the scaffold [6,7].

A number of fabrication techniques have been developed over the years for manufacturing porous bioceramics. These include, amongst others, the replication of polymer foams by ceramic dip coating [8,9] or impregnation, foaming of aqueous ceramic powder suspensions [10,11], pyrolysis of preceramic precursors [12] and firing of ceramic powder compacts with pore-forming fugitive phases [13,14]. However, none of these methods can completely satisfy all the necessary requirements, namely, a controlled level of interconnected porosity combined with good mechanical properties (strength in the region of 20 MPa with a porosity >50%). An example is the foam replication

* Corresponding author. Tel.: +44 1225 386163; fax: +44 1225 386928.
E-mail address: I.G.Turner@bath.ac.uk (I.G. Turner).

1742-7061/$ - see front matter © 2008 Acta Materialia Inc. Published by Elsevier Ltd. All rights reserved.
doi:10.1016/j.actbio.2008.11.009

method, which can achieve very high volumes of porosity and excellent interconnectivity levels but characteristically results in poor mechanical properties due to defects generated during the pyrolysis of the polymer foam template [9].

An alternative approach is to use the freeze-casting (or freeze-drying) process to produce porous ceramics [15]. This has proven to be an attractive manufacturing method as it allows construction of reticulated porous ceramics on a finer scale and without the polymer burnout stage. This avoids some of the inherent problems currently associated with other manufacturing methods. The process consists of freezing a ceramic slurry, which is usually aqueous based, in a mould at low temperatures, followed by demoulding and vehicle removal by sublimation to obtain a green body [15]. More recently, camphene, which has a melting point of approximately 45 °C, [15–18] has been used successfully as a freezing vehicle, allowing more flexibility in the process as it can be frozen and easily sublimed at room temperature [19–21].

The aim of this study was to explore the application of this method to the production of a highly porous calcium phosphate-based ceramic with aligned, interconnected and graded porosity for tissue engineering purposes and to determine the important variables that control the structural characteristics of the final product.

2. Materials and methods

2.1. Materials

Commercially available hydroxyapatite powder TCP130 ($Ca_{10}(PO_4)_6(OH)_2$) (Thermphos) with an average particle size of six microns was selected. The composition of the ceramic powder before, and the bulk specimens after, sintering were quantitatively assessed using X-ray diffraction (XRD). The XRD spectra were obtained between 20 and 60 (2θ) in 0.02° steps. In order to estimate the phase compositions, the Rietveld refinements were performed using a software package "Fullprof Suite" on a 2θ range between 21° and 36° using structural models for the phases identified, including HA, α-tricalcium phosphate (TCP) and β-TCP. Camphene ($C_{10}H_{16}$), 95% purity, Sigma–Aldrich Company Ltd., Gillingham, UK) was used as the freezing vehicle without any further purification. In addition, Texaphor 963 (Cognis, Southampton Hampshire, UK) was used as dispersant (density at 20 °C of 0.89–0.91 gcm^{-3} and acid value of 55–58 mg KOH g^{-1}). The dispersant concentration was 6–100 wt.% of the calcium phosphate powder for all 10, 20 and 30 vol.% of solid loadings.

2.2. Solidification study

The solidification of the slurry was monitored by preparing an HA/Camphene slurry at 60 °C with a solid loading of 2 vol.% and placing a drop into a pre-heated slide glass (both top and bottom) in order to avoid rapid freezing. A low concentration of HA was used in order for the slurry to be sufficiently translucent for analysis under the light microscope. The drop was left to freeze at room temperature, after which the structure formed was examined using optical microscopy, with particular emphasis on observing the presence of primary and secondary dendrites.

2.3. Fabrication methods for bulk samples

The first part of the manufacturing process involved the slurry preparation. This was achieved by melting the camphene at a temperature of 60 °C on a heating plate to create a clear and fluid vehicle. The dispersant concentration was 6–100 wt.% of calcium phosphate powder for all solid loadings. The HA powder was then added in quantities of 10, 20 and 30 vol.%. The slurry was stirred via the use of a motor and stirrer with a cap on the top to prevent any camphene vapour escaping. The slurry was left to stir at a constant temperature for 3 h, for all solid loadings, before pouring into metallic moulds for freezing; the moulds were 15 mm in internal diameter and 80 mm in height. Some samples were left to cool at room temperature (20 °C) for 30 min; other samples were cooled at different temperatures (4 and 30 °C) for the same length of time to study the effect of cooling rate on the solidification characteristics. After solidification, the green body was removed from the moulds and left to sublime (optimised to 20 h) at room temperature in order to remove the camphene entirely and achieve a highly porous structure. Following sublimation, sintering of the green body at 1280 °C enabled the densification of the samples and concomitant improvements in mechanical strength. The sintering regime entailed heating the samples at 35 °C h^{-1} up to 600 °C followed by 1 h of dwell time. They were then heated at 60 °C h^{-1} up to 1280 °C and held at this temperature for 4 h, before cooling down to room temperature at a rate of 120 °C h^{-1}. Prior to sintering, the ceramic powder was 100% HA. Post-sintering, XRD analysis confirmed that the composition of the ceramic body changed to 75% HA, 18% β-TCP and 7% α-TCP.

2.4. Pore structure analysis

The fabricated samples were characterised by evaluating their pore structures, including pore size and porosity, and by observing the densification of the HA/TCP walls using scanning electron microscopy (SEM; JSM 6480LV). The porosity was calculated using mass and volume measurements (using electronic balance and callipers) to determine the density of the porous samples and then comparing this to that of the fully dense ceramic, using a value from the literature of 3.16 g cc^{-1} [22], to find the percentage of "void" (15 samples per condition were examined and standard deviation calculated accordingly). Pore size was determined by measuring the average size of pores from the SEM micrographs taken at four points on each sample 3 mm from the outer wall at a 90° plane (two samples per condition and four locations per sample).

2.5. Compressive strength measurements

For the compressive strength measurements, samples with a diameter of 10 mm and a height of 15 mm were loaded with a crosshead speed of 10 mm min^{-1} using a screw-driven load frame (Instron 3369, Instron Corp.). The stress and strain responses were monitored; in excess of nine samples in each group of 10, 20 and 30 vol.% solid loadings were tested to obtain average values and standard deviations.

3. Results and discussion

3.1. Camphene solidification observations

The solidification of the slurry was studied in order to acquire an understanding of the geometry and characteristics of dendrite formation. Fig. 1a shows the development of dendritic branches (at the extreme of the sample) along the freezing plane, which, in the image, runs towards the top left corner (as indicated by the arrow). Although preheating of both the top and bottom slide glass was used to facilitate two-dimensional dendritic formation, there was still a variance in the temperature gradient posed by the low conductivity of the glass which could explain the difficulty in the development of secondary dendrites at the extremes of the sample. Fig. 1b shows the interconnectivity of the camphene side-branches in the central region of the slide where the temperature gradient was sufficiently high to stimulate secondary dendritic formation but at the same time not too high to favour only primary dendrites. In both instances the HA powder (pre-sintered) is finely dispersed in the background (2 vol.%) and only the solute-rich area adjacent to the dendrites can be observed together with the translucency of the camphene. These observations show the morphology of the dendrites that are produced during the solidification of the camphene and the important role of the heat transfer gradient on determining the final shape and orientation.

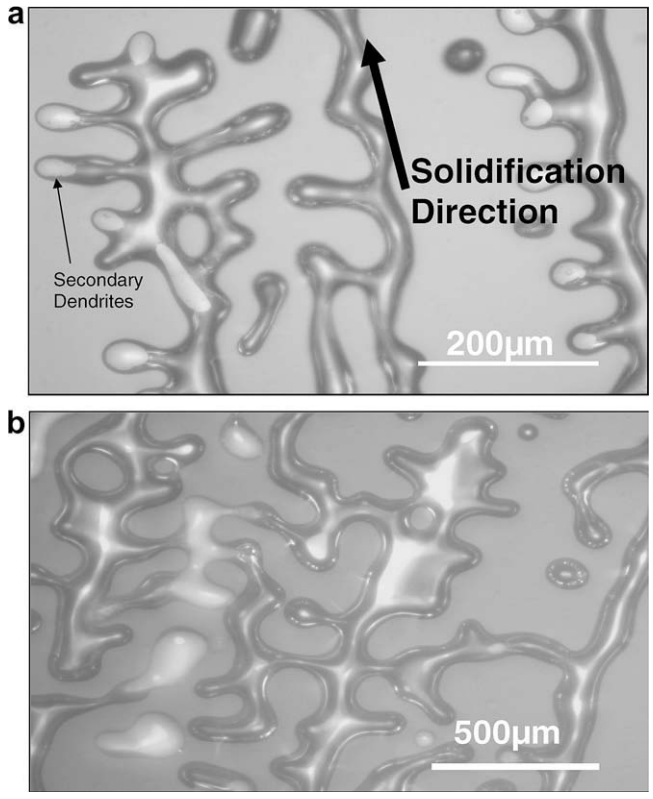

Fig. 1. (a) Solidification of camphene dendrites; (b) interconnection of camphene side-branches.

3.2. Graded porosity observations

Sintered samples generated with solid loadings of 10–30 vol.% were analysed by SEM. The SEM micrographs (Fig. 2a and b) showed that the pores tend to align in the direction of freezing, indicating the possibility of controlling pore orientation by controlling parameters such as the heat transfer gradient and direction of freezing. Fig. 2b shows the three distinct regions that were

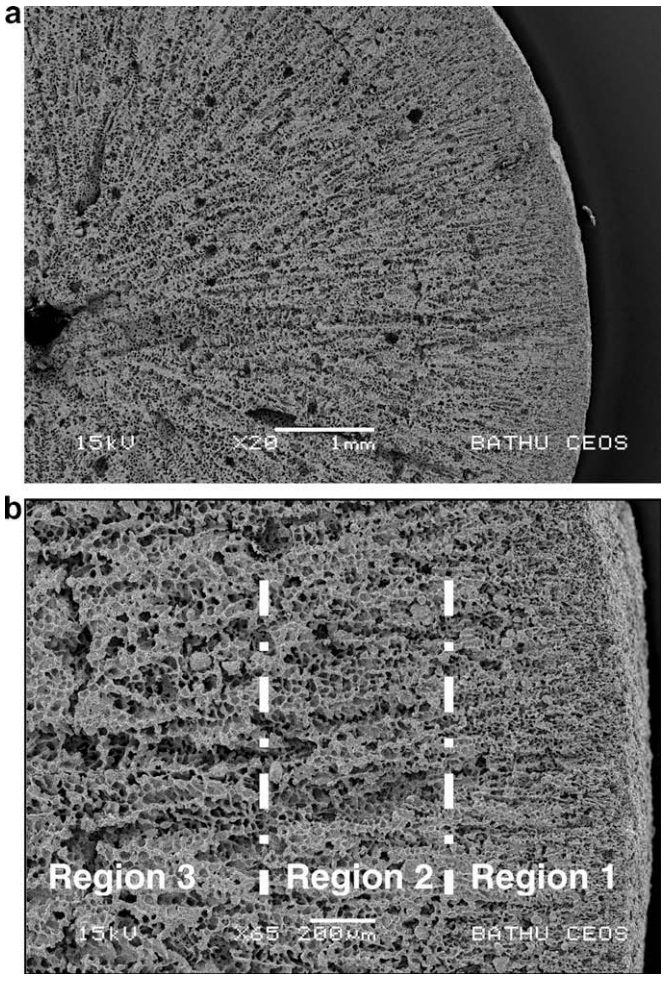

Fig. 2. (a) Pore alignment in the direction of freezing; (b) graded porosity with three distinct regions.

observed, with a denser structure on the outside of the sample, which freezes first, gradually becoming more porous towards the centre of the sample, where the effective heat transfer gradient was lower. This was a qualitative assessment of the change in porosity based on visual observation.

The main heat transfer mechanism in this solidification process is conduction and is governed by the following equation:

$$\frac{\Delta Q}{\Delta t} = -kA\frac{\Delta T}{\Delta x} \quad (1)$$

where A is the cross-sectional surface area, k is the heat transfer coefficient, ΔT is the temperature difference between the ends and Δx is the distance between the ends.

From Eq. (1) it is possible to see the dependence of distance (Δx) on the heat transfer rate ($\Delta Q/\Delta t$), which, in the specific freezing conditions used, is equivalent to the radial direction in the cross-sectional plane of the samples. As the radial distance increases towards the centre of the sample the heat transfer rate reduces, enabling the camphene dendrites to develop larger primary dendritic branches, resulting in greater porosity after sublimation and subsequent sintering.

3.3. Sublimation of the camphene during solidification

The weight loss of the green body during freezing was studied in order to have a better understanding of the processes that occur during the solidification of the slurry. The warm slurry was poured in a cylindrical split mould

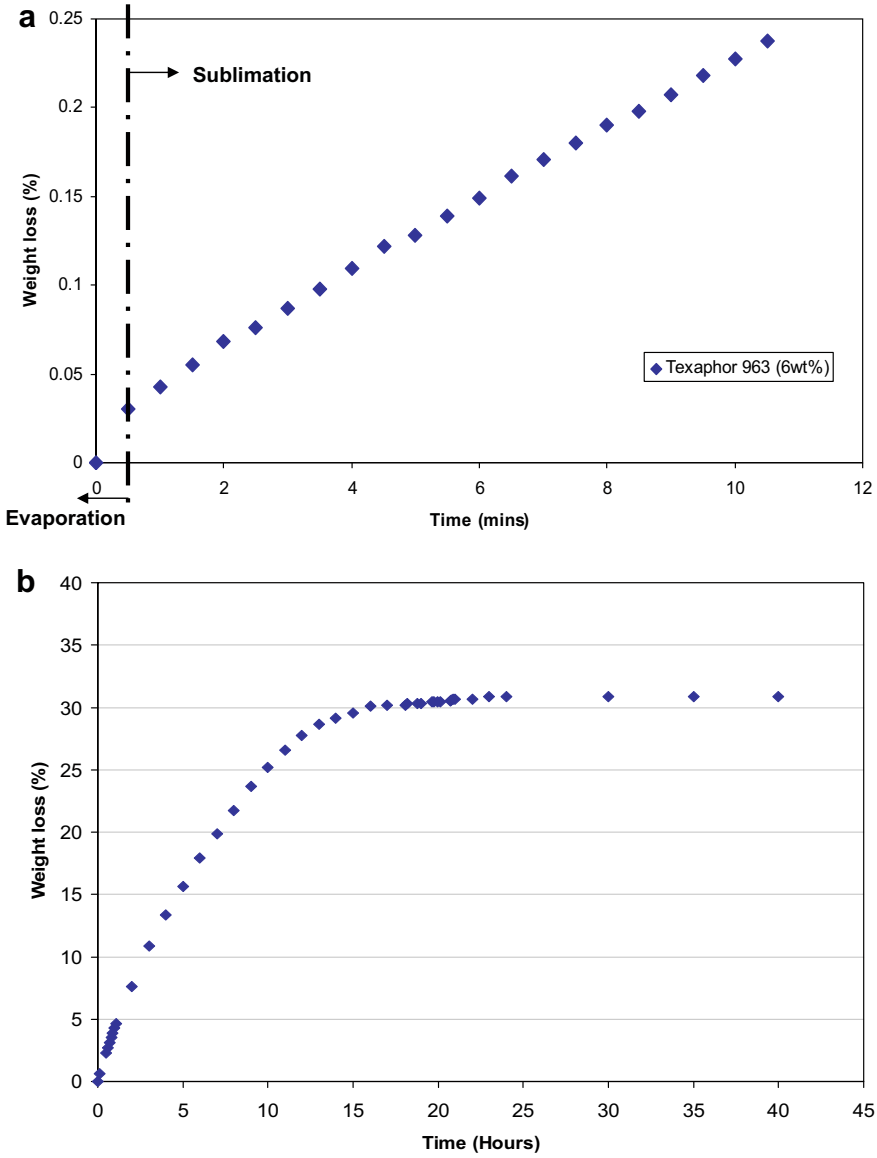

Fig. 3. (a) Weight loss of slurry during solidification of the camphene; (b) weight loss of green body during sublimation of the camphene (30 vol.% solid loading).

with an open top and placed on a weighing scale, and its weight recorded at regular time intervals. Two distinct regions were observed when monitoring the weight loss of the samples (Fig. 3a). In the very early stages (<1 min) there is a rapid increase in weight loss, suggesting that evaporation of the molten camphene dominated

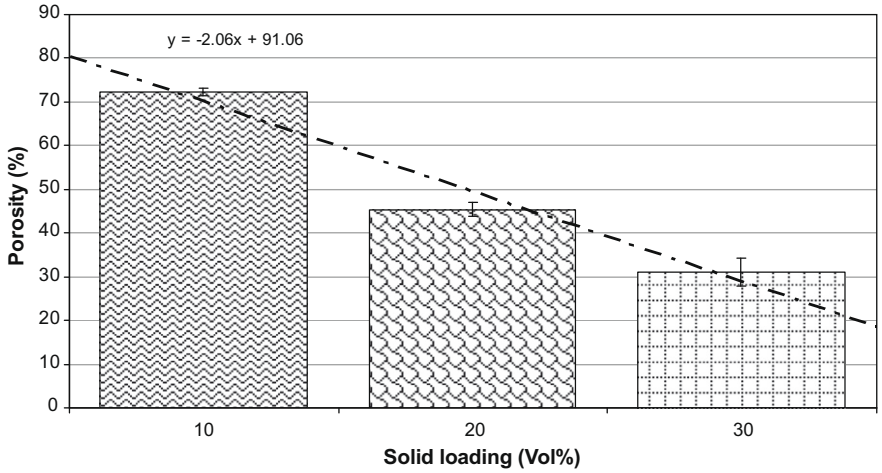

Fig. 4. Porosity variation with solid loading (samples sintered at 1280 °C).

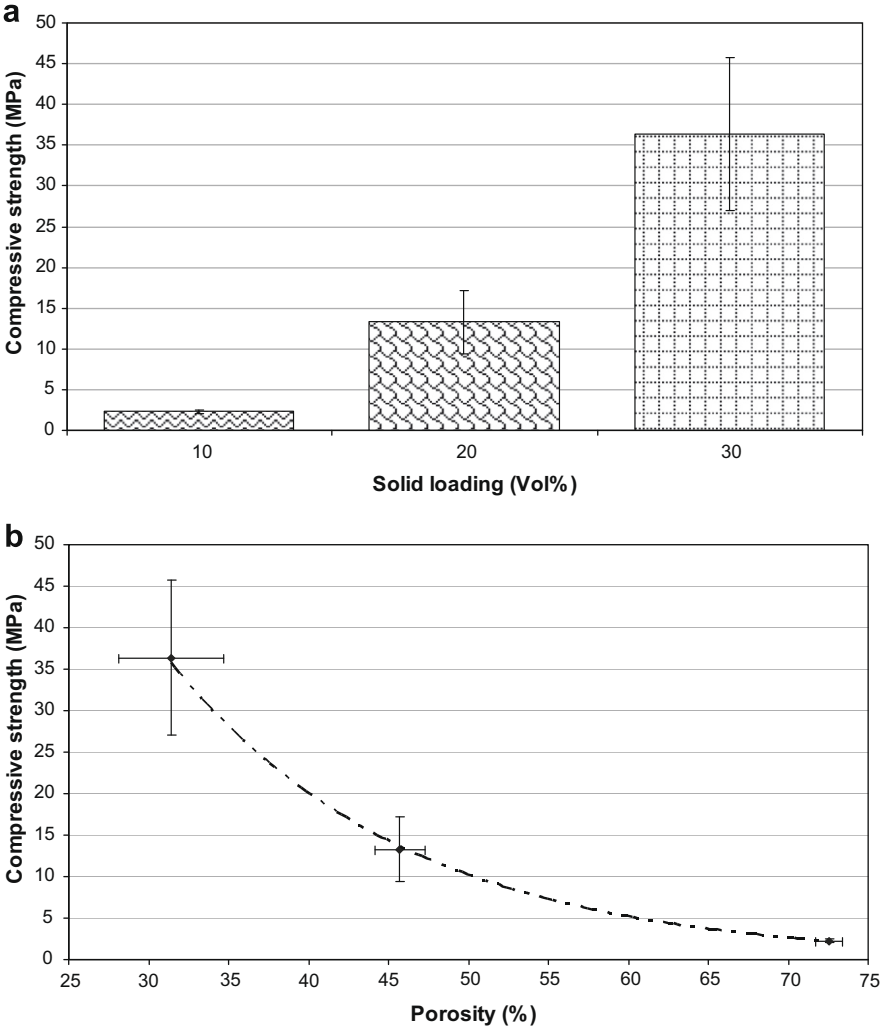

Fig. 5. (a) Effect of solid loading on the compressive strength of sintered samples; (b) the effect of porosity on the compressive strength.

the overall weight loss. The second region is dominated by sublimation as the rate of weight loss is reduced and remains relatively constant thereafter.

3.4. Sublimation of the camphene during the dry-freezing process

Fig. 3b shows the behaviour of the camphene during sublimation as a function of time. The weight loss, shown as a percentage, represents the amount of camphene that is slowly sublimed at room temperature with time. It can be seen that the weight loss has an exponential behaviour with an initially high rate of sublimation for the first 5 h of the process, after which the rate starts to gradually reduce as the quantity of residual camphene begins to diminish. The dry-freezing process took an average of 25 h to complete in an open air environment at room temperature and with a constant flow of air. This time was reduced when the samples were placed in a vacuum for 2 h reducing the length of the process to 20 h. However, it must be noted that the effectiveness of the vacuum is reduced as the concentration of camphene in the environment increases. No shrinkage was observed after complete sublimation of the camphene. However, after sintering a linear shrinkage of about 30% was observed.

3.5. Effect of solid loading on sintered materials

Solid loading plays a critical role in determining the porosity and mechanical strength characteristics of the sin-

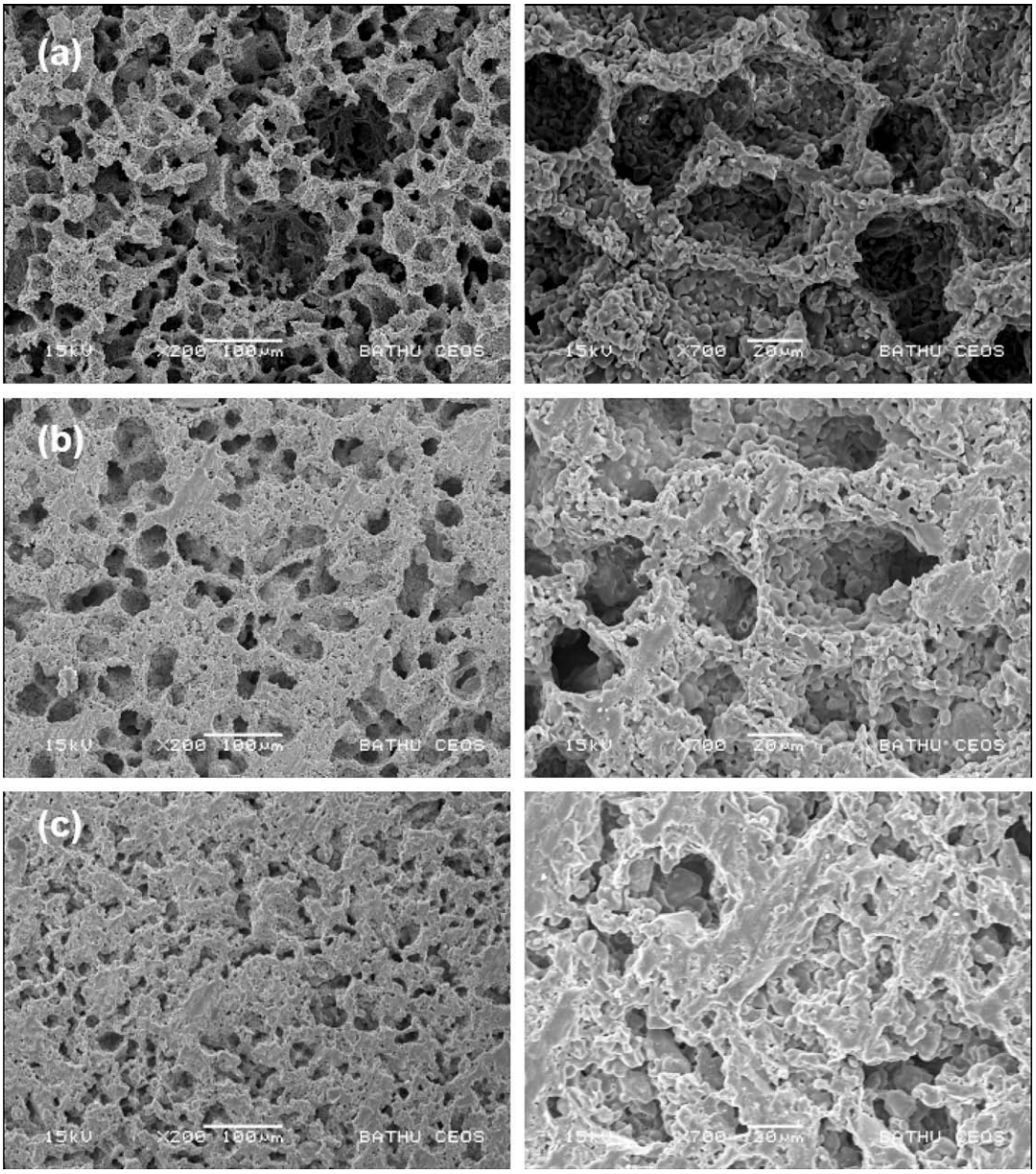

Fig. 6. SEM micrographs of porous structures for (a) 10 vol.%, (b) 20 vol.% and (c) 30 vol.% at 23 °C.

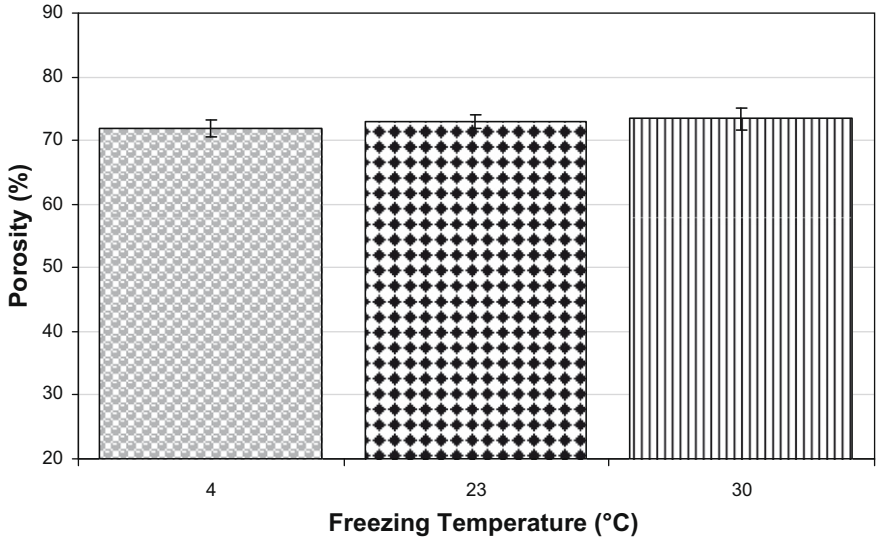

Fig. 7. Graph illustrating the effect of freezing temperature on porosity for 10 vol.% solid loading.

tered samples. Fig. 4 shows how porosity is affected by the initial solid loading of the ceramic slurry. As the solid loading is increased, the porosity was observed to decrease proportionately. The porosity was reduced from 72.5 to 31.4% by increasing the solid loading from 10 to 30 vol.%. The linear relationship between porosity and solid loading can be expressed by the equation:

$$Y = 91.06 - 2.06x \quad (2)$$

where Y is the porosity (vol.%) and x is the solid loading (vol.%).

This result suggests that it is possible to achieve a dense product after sintering with an initial solid loading of 44.2 vol.%. It also shows how the porosity can be manipulated by controlling the solid loading of the slurry.

In addition to porosity level, the solid loading affects the compressive strength of the sintered samples. The compressive strength was increased from 2.3 to 36.4 MPa by increasing the solid loading from 10 to 30 vol.% (Fig. 5a) for samples prepared at room temperature (23 °C). The compressive strength of these materials lies within, or even exceeds, the compressive strength of cancellous bone, which has been reported to be in the range 4–12 MPa [23]. Plotting compressive strength against porosity allows comparison of the general behaviour of the samples and examination of the fundamental limitations posed by the level of porosity on the mechanical strength (Fig. 5b). The error bars indicate the standard deviation of the results recorded. The exponential relationship between compressive strength and porosity shown in Fig. 5b can be expressed by the equation:

$$y = 294.18e^{-6.71x} \quad (3)$$

where y is the compressive strength (MPa) and x is the porosity volume fraction (0–1).

Fig. 6 shows SEM micrographs of the sintered microstructures generated and how these vary with solid loading. A larger porosity and pore size can be seen at low solid loadings as compared to high solid loadings. Samples with 10% solid loading had an average pore size of 100–200 μm, those with 20% solid loading had an average pore size of 40–80 μm and those with 30% solid loading an average pore size of <40 μm.

3.6. Effect of freezing temperature

The effect of freezing temperature on porosity and compressive strength were studied by freezing the camphene-based ceramic slurry at temperatures of 4, 23 and 30 °C. It followed that, whilst the heat transfer gradient does not have much effect on the overall level of porosity (Fig. 7), it does have an effect on pore size distribution and alignment (Fig. 8). Although the overall effect is difficult to quantify in this preliminary study, the results suggest that samples produced at 4 °C had a average pore size of <40 μm, those produced at 23 °C an average pore size of 40–80 μm and those produced at 30 °C an average pore size of >100 μm. As a consequence, the compressive strength of the samples increased from 1.95 to 2.98 MPa by decreasing the freezing temperature from 30 to 4 °C (Fig. 9).

A greater alignment of the pores was observed at lower freezing temperatures due to the larger driving force of the camphene dendrites during the solidification process as a direct consequence of the greater heat transfer gradient (Eq. (1)). However, at higher freezing temperatures and thus low heat transfer rates, the development of larger pores was observed (Fig. 8). This resulted in a more favourable structure for potential osteoblast cell attachment and bone ingrowth.

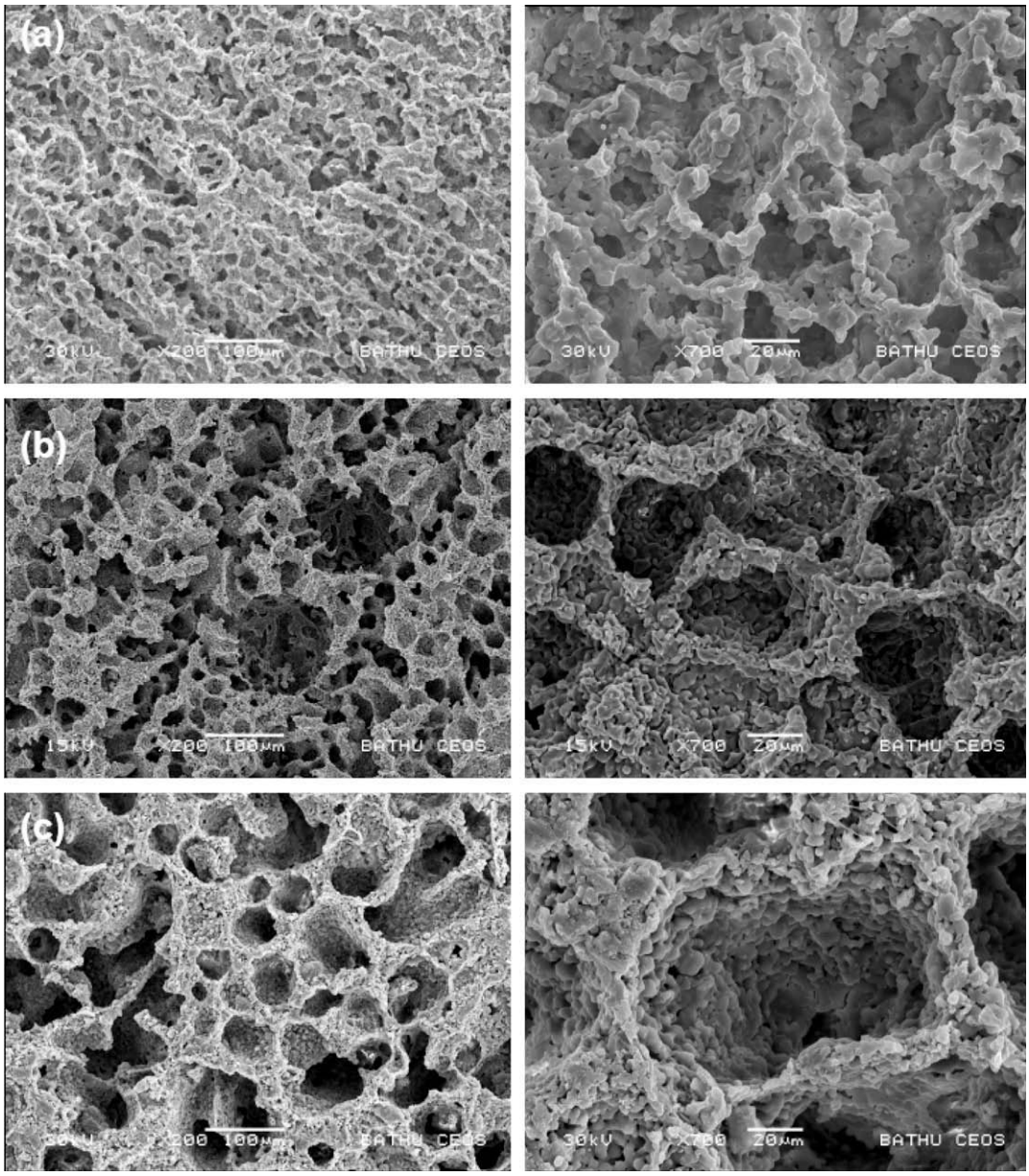

Fig. 8. SEM micrographs showing pore size at freezing temperatures of: (a) 4 °C, (b) 23 °C and (c) 30 °C at 10 vol.% solid loading.

4. Conclusions

It has been demonstrated that large pore channels can be achieved using the novel manufacturing technique of freeze-casting, indicative of the potential for porous HA/TCP scaffolds to be produced using this technique. Initial solid loading played a primary role in the resulting porosity of the scaffolds. This was reduced from 72.5% to 31.4% by increasing the solid loading from 10 to 30 vol.%. As a result of this, the compressive strength was affected, increasing from 2.3 to 36.4 MPa for the respective increase in solid loading.

Camphene dendrites were found to orient according to the direction of freezing; the rate of heat transfer played an important role in the morphology of the dendrites. The freezing temperature affected the pore size distribution rather than the overall percentage porosity, which is believed to be determined mainly by the initial solid loading. Freezing at 4 °C resulted in a greater compressive strength compared to the higher temperatures of 23 and 30 °C. The compressive strength increased from 1.95 to 2.98 MPa when the freezing temperature was decreased from 30 to 4 °C.

No shrinkage was observed after sublimation of the samples prior to sintering, making it a very competitive process relative to, for example, the classical water based ceramic slip that experiences shrinkage during drying, which may result in crack formation and defects within the structure even prior to sintering.

In conclusion, this manufacturing technique shows great potential for generating defect-free scaffolds with con-

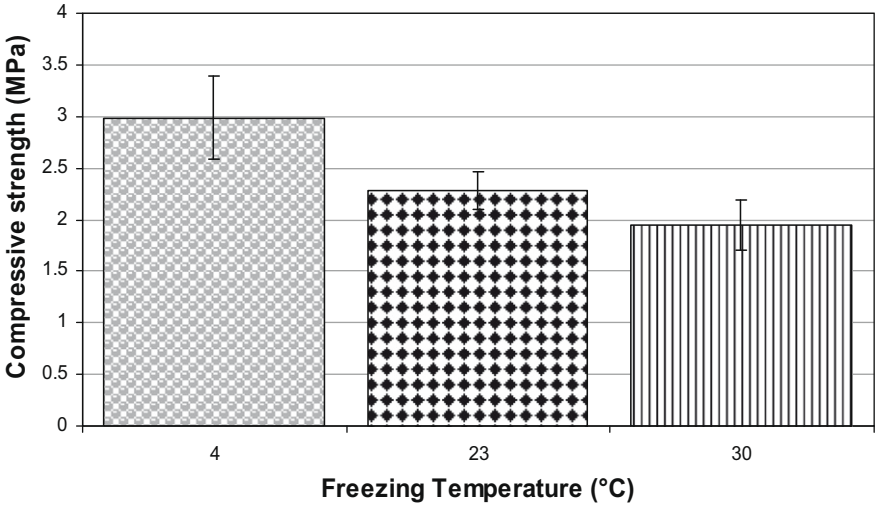

Fig. 9. Effect of freezing temperature on compressive strength for 10 vol.% solid loading.

trolled porosity and pore size and appropriate compressive properties for use in tissue engineering applications.

Acknowledgements

The authors thank the University of Bath for provision of a University studentship for A Macchetta and the Electron Optics Unit for use of their facilities.

References

[1] Padilla S, Sanchez-Salcedo S, Vallet-Regi M. Bioactive and biocompatible pieces of HA/sol–gel glass mixtures obtained by the gel-casting method. J Biomed Mater Res 2005;75A(1):63–72.
[2] Suchanek W, Yoshimura M. Processing and properties of hydroxyapatite- based biomaterials for use as hard tissue replacement implants. J Mater Res 1998;13(1):94–117.
[3] Hench LL, Wilson J. Surface-active biomaterials. Science 1984;226:630–6.
[4] Yuan H, Kurashina K, de Bruin JD, Li Y, de Groot k, Zhang X. A preliminary study on osteoinduction of two kinds of calcium phosphate ceramics. Biomaterials 1999;20:1799–806.
[5] Komlev VS, Barinov SM. Porous hydroxyapatite ceramics of bimodal pore size distribution. J Mater Sci Mater Med 2002;13:295–9.
[6] Hing KA, Best SM, Tanner KE, Bonfield W, Revell PA. Quantification of bone ingrowth within bone-derived porous hydroxyapatite implants of varying density. J Mater Sci Mater Med 1999;10:663–70.
[7] Murphy WL, Simmons CA, Kaigler D, Mooney DJ. Bone Regeneration via a mineral substrate and induced angiogenesis. J Dent Res 2004;83(3):204–10.
[8] Schwartzwalder K, Somers AV. Method of making porous ceramic article. US Patent No. 3, 090094; 1963.
[9] Jun IK, Koh YH, Song JH, Lee SH, Kim HE. Improved compressive strength of reticulated porous zirconia using carbon coated polymeric sponge as novel template. Mater Lett 2006;60(20):2507–10.
[10] Tuck C, Evans JRG. Porous ceramics prepared from aqueous foams. J Mater Sci Lett 1996;18:1003–5.
[11] Pradhan M, Bhargava P. Effect of sucrose on fabrication of ceramic foams from aqueous slurries. J Am Ceram Soc 2005;88(1):216–8.
[12] Schmidt H, Koch D, Grathwohl G. Micro/macro-porous ceramics from preceramic precursors. J Am Ceram Soc 2005;84:2252–5.
[13] Lyckfeldt O, Ferreira JMF. Processing of porous ceramics by starch consolidation. J Eur Ceram Soc 1998;18:131–40.
[14] Boaro M, Vohs JM, Gorte RJ. Synthesis of highly porous yttria-stabilised zirconia by tape casting methods. J Am Ceram Soc 2003;86(3):395–400.
[15] Yoon BH, Koh YH, Park CS, Kim HE. Generation of large pore channels for bone tissue engineering using camphene-based freeze casting. J Am Ceram Soc 2007;90(6):1744–52.
[16] Koh YH, Lee EJ, Yoon BH, Song JH, Kim HE. Effect of polystyrene addition on freeze casting of ceramic/camphene slurry for ultra high porosity ceramics with aligned pore channels. J Am Ceram Soc 2006;89(12):3646–53.
[17] Koh YH, Song JH, Lee EJ, Kim HE. Freezing dilute ceramic/camphene slurry for ultra high porosity ceramics with completely interconnected pore networks. J Am Ceram Soc 2006;89(10):3089–93.
[18] Yoon BH, Lee EJ, Kim HE, Koh YH. Highly aligned porous silicon carbide ceramics by freezing polycarbosilane/camphene solution. J Am Ceram Soc 2007;90(6):1753–9.
[19] Lee EJ, Koh YH, Yoon BH, Kim HE, Kim HW. Highly porous hydroxyapatite bioceramics with interconnected pore channels using camphene-based freeze casting. Mater Lett 2007;61:2270–3.
[20] Araki K, Halloran JW. Porous ceramic bodies with interconnected pore channels by a novel freeze casting technique. J Am Ceram Soc 2005;88(5):1108–14.
[21] Song JH, Koh YH, Kim HE. Fabrication of a porous bioactive glass-ceramic using room temperature freeze casting. J Am Ceram Soc 2006;89(8):2649–53.
[22] Simske SJ, Ayers RA, Bateman TA. Porous materials for bone engineering. Mater Sci Forum 1997;250:151–82.
[23] Yang S, Leong KF, DU Z, Chua CK. The design of scaffolds for use in tissue engineering. Part I. Traditional factors. Tissue Eng 2001;7(6):679–89.